

Dalton Transactions

An international journal of inorganic chemistry

Accepted Manuscript

This article can be cited before page numbers have been issued, to do this please use: M. Mazur, M. Mrozowicz, W. Buchowicz, M. Koszytkowska-Stawinska, R. Kaminski, Z. Ochal, P. Wiska and M. Bretner, *Dalton Trans.*, 2020, DOI: 10.1039/D0DT01975E.



This is an Accepted Manuscript, which has been through the Royal Society of Chemistry peer review process and has been accepted for publication.

Accepted Manuscripts are published online shortly after acceptance, before technical editing, formatting and proof reading. Using this free service, authors can make their results available to the community, in citable form, before we publish the edited article. We will replace this Accepted Manuscript with the edited and formatted Advance Article as soon as it is available.

You can find more information about Accepted Manuscripts in the [Information for Authors](#).

Please note that technical editing may introduce minor changes to the text and/or graphics, which may alter content. The journal's standard [Terms & Conditions](#) and the [Ethical guidelines](#) still apply. In no event shall the Royal Society of Chemistry be held responsible for any errors or omissions in this Accepted Manuscript or any consequences arising from the use of any information it contains.

Formylation of a metathesis-derived *ansa*[4]-ferrocene: a simple route to anticancer organometallics

View Article Online
DOI: 10.1039/D0DT01975E

Maria Mazur,^[a] Michał Mrozowicz,^[a] Włodzimierz Buchowicz,^{*[a]} Mariola Koszytkowska-Stawińska,^[a] Radosław Kamiński,^[b] Zbigniew Ochal,^[c] Patrycja Wińska,^[c] Maria Bretner^[c]

^[a] Faculty of Chemistry, Chair of Organic Chemistry, Warsaw University of Technology, Noakowskiego 3, 00-664 Warsaw, Poland

^[b] Department of Chemistry, University of Warsaw, Żwirki i Wigury 101, 02-089 Warsaw, Poland

^[c] Faculty of Chemistry, Chair of Drug and Cosmetics Biotechnology, Warsaw University of Technology, Noakowskiego 3, 00-664 Warsaw, Poland

Abstract

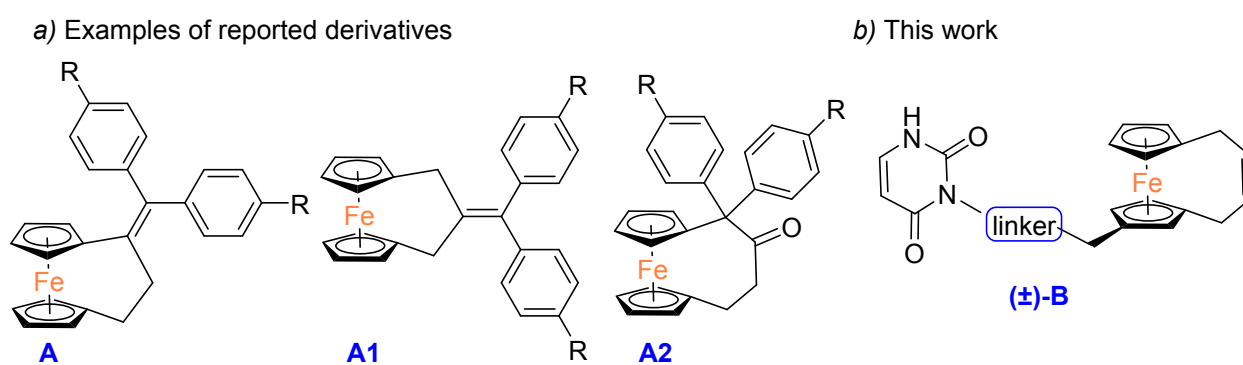
Formylation of *ansa*[4]-ferrocene, obtained through the ruthenium-catalysed olefin metathesis, yields two separable, planar chiral 1,3- and 1,2-*ansa*-ferrocene aldehydes. Single-crystal X-ray structure analysis reveals that both regioisomers crystallize with spontaneous resolution of the racemate in the chiral $P2_12_12_1$ space group with one molecule in the asymmetric unit. The major 1,3-isomer was further transformed into a conjugate with 1,2,3-triazole and uracil using the “click” chemistry as the key synthetic step. This inorganic-organic hybrid displays anticancer activity (MCF-7, A549, MDA-MB-231 cell lines) with EC_{50} values comparable to those for cisplatin.

1. Introduction

Ansa[*n*]-ferrocenes ([*n*]ferrocenophanes) are defined as iron complexes having the two cyclopentadienyl rings connected by a bridge with variable length and structure ([*n*] denotes the number of bridging atoms). A considerable variety of ferrocenophanes have been synthesized up to date using different routes, to name among others the original “fly-trap” method.¹ Moreover, since the seminal reports by Locke *et al.*^{2a} and Ogasawara *et al.*,^{2b} alkene

metathesis in the metal coordination sphere has been recognized as a useful tool in the synthesis of these compounds. Metathesis-derived *ansa*-metallocenes exhibit low ring-tilt and a rigid bridge, and thus in many aspects resemble properties and reactivity of the parent metallocenes.^{3,4}

While numerous ferrocene derivatives were known to display promising biological activity,^{5,6} the potential of *ansa*-ferrocenes in medicinal chemistry has been discovered recently. A series of bridge-functionalized [3]ferrocenophanes (Scheme 1a) with activity against cancer-cell lines was obtained using the McMurry cross-coupling reactions.⁷ Since Plažuk *et al.* recognized that the ferrociphenol analogue (Scheme 1a, compound **A**, R = OH) is more potent than its regioisomer **A1**^{7a} or the transposition product **A2**,^{7e} much attention has been paid to structural modifications of compounds **A**. The examination of several derivatives **A** in terms of their cytotoxicity against hormone-independent MDA-MB-231 breast cancer cells revealed that many of them displayed higher activity when compared to their flexible, non-bridged analogues. This superiority was attributed to the rigid shape of the ferrocenophanes which allows for their tight binding to a receptor, providing the molecules possess the proper geometry.



Scheme 1. (a) Previous work, bridge-substituted [3]ferrocenophanes **A**, **A1**, and [4]ferrocenophanes **A2** with cytotoxic activity (R = H, OH, NH₂, NHAc, Br, CN, NHC(O)(CH₂)₆C(O)NHOH).⁷ (b) This work, the target ring-substituted, metathesis-derived [4]ferrocenophanes **(±)-B**.

The limited synthetic scope of compounds **A** encouraged us to develop a straightforward ring-functionalization of a metathesis-derived *ansa*[4]-ferrocene as a facile route to novel conjugates with biologically relevant molecules, such as uracil (Scheme 1b, compound **B**). Since ferrocenecarboxaldehyde has been successfully used in the development of numerous ferrocene bioconjugates,⁸ we focused our synthetic attempts on a formyl group as a versatile entry into further connection with diverse building blocks. In the light of reports on anticancer activity of compounds **A**, we were interested in evaluation of cytotoxic activity of the target compounds **B**.

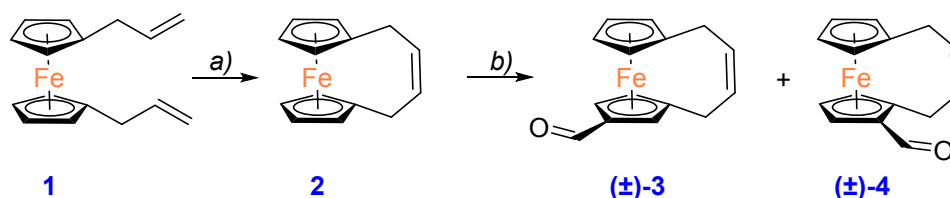
2. Results and Discussion

2.1. Synthesis and spectroscopic characterization

Ring-monosubstitution of a ferrocenophane in most cases yields two regioisomeric 1,3- and 1,2-products (or β and α isomers), and results in molecules displaying planar chirality.⁹ Moreover, several disubstituted products could be also formed that usually were difficult to identify and isolate. Consequently, reports on successful ring-functionalization of *ansa*-ferrocenes have been rather limited. Notable examples include the Friedel-Crafts acetylation of [*n*]ferrocenophanes ($n = 3-5$) with acetyl chloride/ AlCl_3 ,¹⁰ formylation of [*n*]ferrocenophanes ($n = 3-4$) or multibridged ferrocenophanes with DMF/ POCl_3 ,¹¹ lithiation of 1,1'-trimethyleneferrocene with *n*-BuLi/TMEDA,¹² mercuration with subsequent halogenation,¹³ and borylation with BBr_3 .¹⁴ While in most reactions the β -isomer predominates for steric reasons, the directed *ortho* metalation of a dimethylamino-substituted [3]ferrocenophane provided selective route to the α -isomer.¹⁵ Taking into account those reports, in particular the slow lithiation of 1,1'-trimethyleneferrocene,¹² we focused our attempts on the formylation under the Friedel-Crafts conditions reported for ferrocene.¹⁶

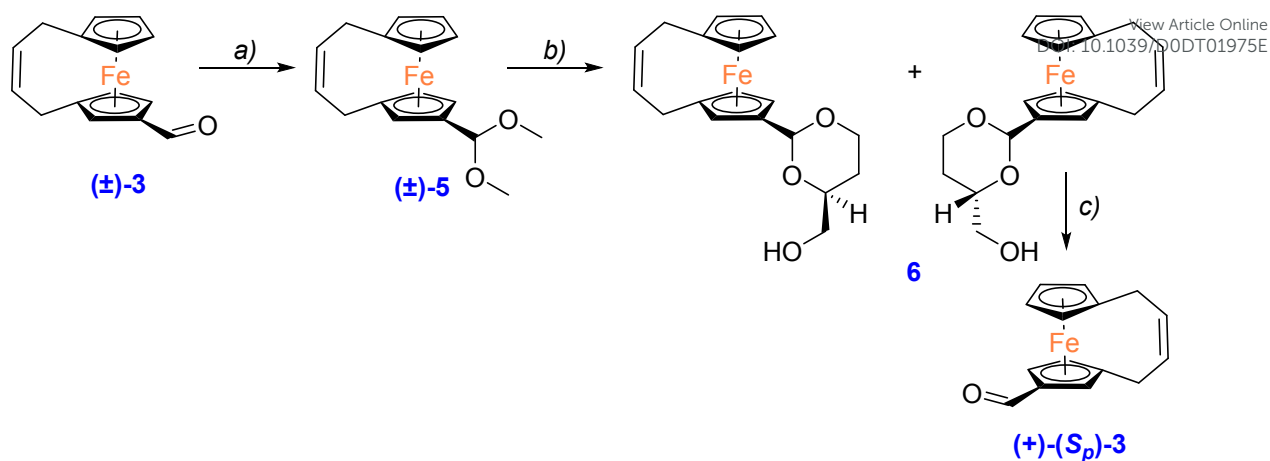
1,1'-Diallylferrocene (**1**) readily undergoes ring-closing metathesis in the presence of the first generation Grubbs catalysts to form ferrocenophane **2** in high yield, exclusively as the

Z-isomer.² Reactions of **2** with triethyl orthoformate and AlCl₃ at room temperature cleanly afforded two aldehydes, as judged from the ¹H NMR spectra of the crude reaction mixtures (major CHO resonance at $\delta = 9.81$ ppm, minor at $\delta = 10.07$ ppm). The ratio of these two products varied slightly from 3.3:1 to 2.9:1 in some consecutive runs. Thus, we tested also the Vilsmeier reaction (DMF/POCl₃)^{17,11c} to obtain the same products at the 4:1 ratio (Scheme 2).



Scheme 2. Synthesis of the (±)-**3** and (±)-**4** aldehydes: (a) [Ru(=CHPh)Cl₂(PCy₃)₂], CH₂Cl₂, reflux, 3 h (ref. 2); (b) CH(OEt)₃, AlCl₃, toluene, 0 °C to rt, 1 h; or DMF, POCl₃, CHCl₃, rt, 20 h.

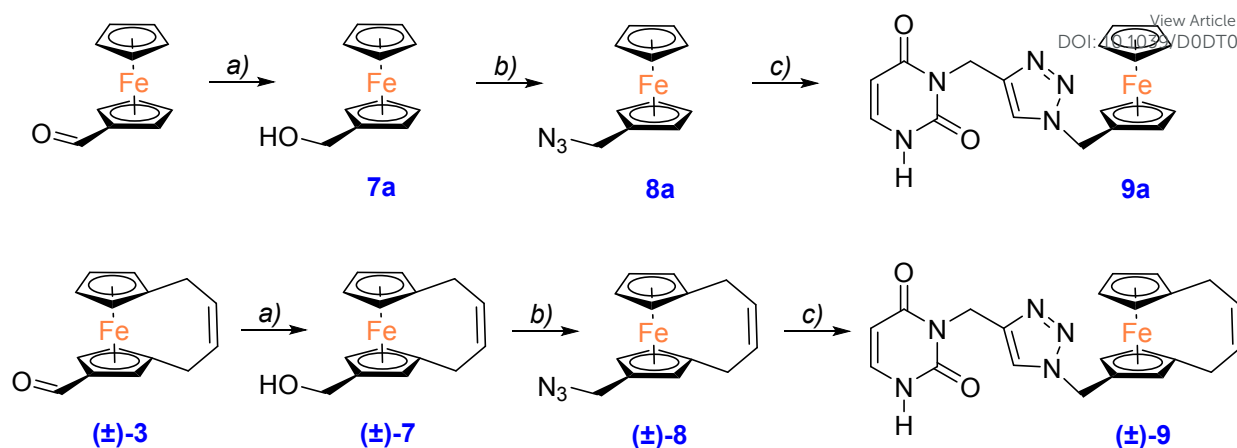
The (±)-**3** and (±)-**4** regioisomers were isolated by column chromatography on silica gel in 47% and 19% yields, respectively, and fully characterized, including X-ray crystallography (Figure 1 and Figure 2, respectively). While the ¹H and ¹³C NMR spectra of **2** are straightforward and feature four and five signals, respectively, incorporation of the ring substituent renders all the proton and carbon atoms inequivalent. Consequently, the NMR spectra of (±)-**3** and (±)-**4** are remarkably complex. Thus, the expected seven cyclopentadienyl proton resonances were clearly observed. Interestingly, the olefinic and allylic protons signals show significantly different patterns allowing to tentatively distinguish the 1,2- and 1,3-isomers (Figure S1 and Figure S2 in the Supporting Information). Both (±)-**3** and (±)-**4** display chiral planarity and were resolved into enantiomers on an analytical Chiralcel OD-H or AD-H column, respectively (Figure S3 and Figure S4). For the preparative resolution of the racemic major product (±)-**3** (Scheme 3), the method originally reported by Kagan and co-workers was adopted.¹⁸



Scheme 3. Resolution of (±)-**3** into enantiomers: (a) $\text{CH}(\text{OMe})_3$, *p*-TsOH, 80-90 °C; (b) (*S*)-(-)-1,2,4-butanetriol, *p*-TsOH, CHCl_3 , 60 °C, then crystallization from hexanes and 2-propanol at 4 °C; (c) *p*-TsOH, CH_2Cl_2 , H_2O , 60 °C.

The dimethyl acetal (±)-**5**, obtained from (±)-**3** and triethyl orthoformate, reacted with commercial (*S*)-(-)-1,2,4-butanetriol in chloroform using catalytic *p*-TsOH to yield the diastereomeric acetals **6**. The two diastereoisomers of **6** were clearly distinguishable with ^1H NMR spectroscopy using the diagnostic O-CH-O signals at $\delta = 5.332$ and $\delta = 5.326$ ppm, and were separated by repeated crystallizations. Acidic hydrolysis of the diastereoisomer that crystallized from hexanes/2-propanol mixtures released the enantiomerically enriched (+)-(*S_p*)-**3** with $[\alpha]_{\text{D}}^{20} = 167.5$ ($c = 0.08$ in CHCl_3).

In an attempt to show that the *ansa*-ferrocene aldehyde (±)-**3** can be used in the synthesis of bio-conjugates analogously to ferrocenecarboxaldehyde, reactions depicted on Scheme 4 were carried out, resulting in inorganic-organic hybrids **9a**¹⁹ and (±)-**9**.



Scheme 4. Synthesis of **9a** and **(±)-9**: (a) NaBH₄, MeOH, THF, rt, 24 h for **7a**, 48 h for **(±)-7**; (b) NaN₃, CH₃COOH, 50 °C, 3 h; (c) 3-propargyluracil, CuSO₄ × 5H₂O, sodium ascorbate, EtOH, rt, 3 days for **9a**, 4 days for **(±)-9**.

The aldehyde **(±)-3** was reduced with NaBH₄ in methanol/THF under conditions similar to those for ferrocenecarboxaldehyde,²⁰ albeit extended reaction time was required. Then, nucleophilic substitution in **(±)-7** with sodium azide in acetic acid afforded the azide **(±)-8**. The Cu(I)-catalysed 1,3-dipolar cycloaddition of the azide with 3-propargyluracil was successfully performed to yield the *ansa*-ferrocene-triazole-uracil conjugate **(±)-9**. The structure of **(±)-7**, **(±)-8** and **(±)-9** was established by NMR, MS, and elemental analyses. Thus, for example the ¹H NMR spectrum of **(±)-9** features the diagnostic uracil doublets of doublets at $\delta = 5.72$ and 7.17 ppm, the triazole singlet at $\delta = 7.53$ ppm, and unresolved olefinic multiplets at $\delta = 5.99$ -6.03 ppm.

2.2. X-ray characterization

Slow crystallization of **(±)-3** and **(±)-4** from hexanes results in spontaneous resolution of the enantiomers. Both compounds crystallize in the chiral *P*2₁2₁2₁ space group with one molecule in the asymmetric unit. The absolute structure determination of the randomly selected crystals leads to (*R_p*)-**3** and (*R_p*)-**4** configuration, as shown in Figure 1 and Figure 2, respectively (for

details see the Supporting Information). Owing to the presence of the bridge, the cyclopentadienyl ligands are forced to adopt an eclipsed conformation (it is known the staggered conformation is more energetically favoured and dominates across the phase diagram of the parent ferrocene).²¹ As expected, the C13=C14 double bonds adopt the (*Z*)-configuration, and the CHO groups lie approximately in the cyclopentadienyl ligand plane (O1–C1–C2–C3/6 torsion angles equal 12.7(15)° and 15.7(7)° for (*R_p*)-**3** and (*R_p*)-**4**, respectively). The angles between the two least-squares planes fitted for the cyclopentadienyl rings show that both molecules are slightly bent towards the bridge (174.00(1)° and 177.25(4)° for (*R_p*)-**3** and (*R_p*)-**4**, respectively). Overall, it can be concluded that the molecules are quite alike in terms of their size and shape. This is reflected in the unit cell parameters for both structures being rather quite similar (Table S1 in the Supporting Information). The overall weak interaction pattern is also similar in both structures. Apart from numerous H...H contacts being present, some more specific C–H...O interactions are formed between the CHO group and the nearest cyclopentadienyl ligands or the alkyl bridge. On the other hand, the location of the CHO group with respect to the bridge in one of the cyclopentadienyl rings results in the packing of the molecules in crystal structures being overall rather different (Figure S7 and Figure S8).

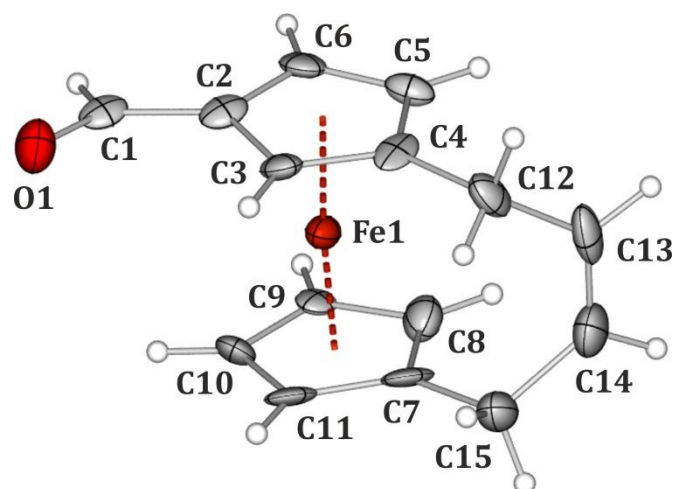


Figure 1. The molecular structure of (*R_p*)-**3**. Atomic thermal motion is represented as ellipsoids (50% probability level), and hydrogen-atom labels are omitted for clarity. View Article Online
DOI: 10.1039/D0DT01975E

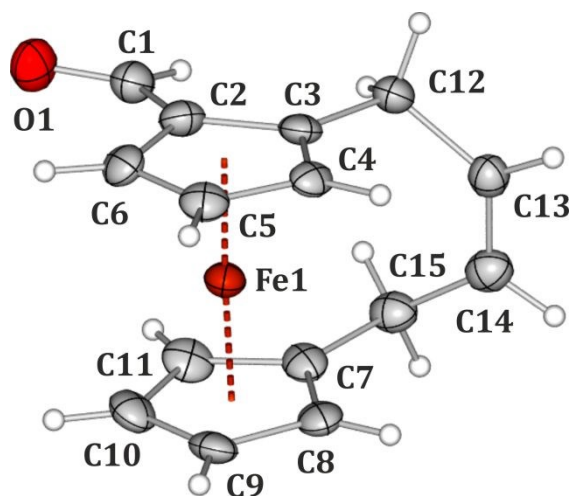


Figure 2. The molecular structure of (*R_p*)-**4**. Atomic thermal motion is represented as ellipsoids (50% probability level), and hydrogen-atom labels are omitted for clarity.

2.3. Biological evaluation

The antitumor activity of newly obtained compounds was evaluated using hormone-dependent human breast carcinoma cell line MCF-7, hormone-independent human breast carcinoma cell line MDA-MB-231, as well as human Caucasian lung carcinoma cell line A549. Normal MRC-5 human fetal lung fibroblasts were used as a reference cell line to study cytotoxicity of these compounds (Table 1, Figure S9). Cisplatin was used as the reference antitumor agent. Ferrocenylmethyl azide **8a** was also tested as a control, and contrary to the reported ferrocenylalkenyl azide (FcCH=CHCH₂N₃),²² showed no activity. Compounds **9a** and (±)-**9**²³ demonstrated antiproliferative activity towards the studied cell lines. In general, the *ansa*-complex (±)-**9** showed lower EC₅₀ values than the unbridged complex **9a**. This observation can be tentatively explained in terms of the rigid structure of (±)-**9**, similarly to the [3]ferrocenophanes reported by Jaouen and co-workers.⁷ The EC₅₀ values determined for compound (±)-**9** towards breast carcinoma cell lines were comparable to those for cisplatin

(MCF-7, 28.7 μM vs 32.9 μM for cisplatin; MDA-MB-231, 30.3 μM vs 23.0 μM for cisplatin)

View Article Online
DOI: 10.1039/D0DT01975E

Moreover, compound (\pm)-**9** exhibited slightly lower activity against A549 cell line than cisplatin (EC_{50} = 10.9 μM vs EC_{50} = 4.6 μM , respectively). Compound (\pm)-**9** with EC_{50} = 45.9 μM also displayed much lower toxicity against normal MRC-5 cells than cisplatin (EC_{50} = 8.4 μM). Consequently, the low cytotoxicity of compound (\pm)-**9** towards MRC-5 cells resulted in higher therapeutic index (defined as a ratio of $\text{EC}_{50}(\text{MRC-5})/\text{EC}_{50}(\text{A549})$) than that for cisplatin.

Table 1. The viability of MCF-7, A549, MDA-MB-231, and MRC-5 cell lines after 72 hours treatment with the newly obtained compounds.

Compound	Cell viability/ $\text{EC}_{50} \pm \text{SD}$ (μM) ^a			
	MCF-7 ^b	A549 ^c	MDA-MB-231 ^d	MRC-5 ^e
8a	189.0	>100	> 200	-
9a	47.7 \pm 1.1	28.5 \pm 2.2	89.6 \pm 7.5	91.8 \pm 4.4
(\pm)- 9	28.7 \pm 2.0	10.9 \pm 1.7	30.3 \pm 4.3	45.9 \pm 1.5
cisplatin	32.9 \pm 0.8	4.6 \pm 1.4	23.0 \pm 4.6	8.4 \pm 0.4

^a EC_{50} values were obtained from a MTT-based assay and an equation of $Y = 100/(1+10^{((\text{LogEC}_{50}-X)*\text{HillSlope}))}$); ^b MCF-7, hormone-dependent human breast carcinoma cell line; ^c A549, human Caucasian lung carcinoma cell line, ^d MDA-MB-231, hormone-independent human breast carcinoma cell line, ^e MRC-5, human fetal lung fibroblasts cell line.

The anticancer activity of (\pm)-**9** and **9a** is comparable to that of ferrocene-modified uracils²⁴ or ferrocene-1,2,3-triazole hybrids.²⁵ [3]Ferrocenophanes **A** and **A1** (Scheme 1a), that represent modifications of polyphenols with well-established cytotoxicity, are significantly more active with IC_{50} values against MDA-MB-231 cells in the nanomolar range.^{7a}

Ferrocene derivatives have recently been suggested as potent anticancer agents owing to their ability to decrease proliferation by inducing senescence in cancer cells.²⁶ To determine the extent of senescence/cell death induced by the most active compounds, *i.e.* (\pm)-**9** and **9a**, β -

galactosidase activity, a senescence marker,²⁷ was detected in MCF-7 cell line. Etoposide, a senescence inducing agent,²⁸ was used as a positive control. The cells were cultured in the presence of gradually increasing concentrations of the compounds (6.25, 12.5, 25 and 50 μM), and assayed for the activity of β -galactosidase after 48 hours of treatment. The examined compounds (\pm)-**9** and **9a** did not induce senescence in MCF-7 cells, in contrast to etoposide (Figure S10). These findings suggest that other factors than the ability to induce senescence in cancer cells play a role in the observed anticancer activity of compounds **9a** and (\pm)-**9**. Identification of these factors needs further studies.

3. Conclusions

We have shown that the *ansa*-ferrocene **2** was regioselectively formylated to give separable, planar-chiral aldehydes (\pm)-**3** and (\pm)-**4** in 66% combined yield. The β -isomer (\pm)-**3** predominated under the tested reaction conditions, most likely for steric factors. It was further transformed in three straightforward synthetic steps into an *ansa*-ferrocene-triazole-uracil conjugate (\pm)-**9** that displayed anticancer activity (MCF-7, A549, and MDA-MB-231 cell lines) with EC_{50} in the micromolar range. Our finding suggests that the activity is most likely related to all structural motifs in bioferrocenes (\pm)-**9** and **9a**. Thus, a family of organometallics with anticancer potential is reported.

4. Experimental

4.1. General Methods

All reactions, except the synthesis of azide (\pm)-**8**, were carried out under an inert atmosphere of argon using Schlenk tube techniques. Solvents were purified by conventional methods.²⁹ 1,1'-Diallylferrocene (**1**),^{2b} 1,1'-(2-buten-1,4-diyl)ferrocene (**2**),² ferrocenemethanol (**7a**),²⁰ azidomethylferrocene **8a**,³⁰ 3-propargyluracil¹⁹ were prepared using published methods. AlCl_3 was sublimed under vacuum. All other compounds were obtained from commercial sources and were used without further purification. The NMR spectra were recorded on a Varian VNMR

500 MHz spectrometer at ambient temperature. The ESI MS were acquired on a Q-TOF Premier or Thermo Q Exactive (TOF HR MS) spectrometers. The optical rotation was measured on an Anton Paar MCP-150 polarimeter; the α value is given in $10^{-1} \text{ deg}\cdot\text{cm}^2\cdot\text{g}^{-1}$, concentration c in $\text{g}/(100 \text{ mL})$. The HPLC analysis were performed on Shimadzu CTO-10ASV chromatograph equipped with a STD-20A UV detector and a Chiralcel OD-H or Chiralcel AD-H chiral column (4.6 mm x 250 mm, from Daicel Chemical Ind., Ltd.) equipped with a pre-column (4 mm x 10 mm, 5 μm). The wavelength of UV detection was set at 254 nm. The HPLC analyses were executed in an isocratic and isothermal (30 $^{\circ}\text{C}$) mode.

4.2. Synthesis of (\pm)-**3** and (\pm)-**4**

Triethyl orthoformate (1.68 mL, 9.90 mmol) and freshly sublimed AlCl_3 (2.26 g, 16.95 mmol) were added to a solution of **2** (390 mg, 1.64 mmol) in dry toluene (15 mL) at 0 $^{\circ}\text{C}$. The reaction mixture was stirred for 1 hour at room temperature, then it was poured into an ice-cold saturated aq. $\text{Na}_2\text{S}_2\text{O}_3$ solution (80 mL). The phases were separated, the aqueous phase was extracted with diethyl ether. The combined organic phases were dried over anhydrous Na_2SO_4 and evaporated to dryness to give orange oil. It was dissolved in hexane and purified by column chromatography on silica gel (hexanes:ethyl acetate 5:1). The first fraction was identified as substrate **2**; then compound (\pm)-**4** (the 1,2-isomer) was eluted: red solid, yield 84.0 mg (0.31 mmol, 19%). ^1H NMR (500 MHz, CDCl_3): δ 2.89-2.94 (m, 1H, $\text{CH}_2\text{-CH=}$), 2.98-3.05 (m, 2H, $\text{CH}_2\text{-CH=}$), 3.63 (ddd, $J = 15.3 \text{ Hz}$, 7.6 Hz, 1.3 Hz, 1H, $\text{CH}_2\text{-CH=}$), 3.96-3.97 (m, 1H, $\text{C}_5\text{H}_3/\text{C}_5\text{H}_4$), 4.00-4.01 (m, 1H, $\text{C}_5\text{H}_3/\text{C}_5\text{H}_4$), 4.20-4.22 (m, 1H, $\text{C}_5\text{H}_3/\text{C}_5\text{H}_4$), 4.24-4.25 (m, 1H, $\text{C}_5\text{H}_3/\text{C}_5\text{H}_4$), 4.44 (t, $J = 2.6 \text{ Hz}$, 1H, $\text{C}_5\text{H}_3/\text{C}_5\text{H}_4$), 4.45 (app. s, 1H, $\text{C}_5\text{H}_3/\text{C}_5\text{H}_4$), 4.65 (dd, $J = 2.6 \text{ Hz}$, 1.5 Hz, 1H, $\text{C}_5\text{H}_3/\text{C}_5\text{H}_4$), 6.02-6.07 (m, 1H, CH=), 6.13-6.18 (m, 1H, CH=), 10.09 (s, 1H, CHO) ppm. ^{13}C $\{^1\text{H}\}$ NMR (126 MHz, CDCl_3): δ 22.2 ($\text{CH}_2\text{-CH=}$), 23.9 ($\text{CH}_2\text{-CH=}$), 68.0 ($\text{C}_5\text{H}_3/\text{C}_5\text{H}_4$), 69.6 ($\text{C}_5\text{H}_3/\text{C}_5\text{H}_4$), 70.3 ($\text{C}_5\text{H}_3/\text{C}_5\text{H}_4$), 71.4 ($\text{C}_5\text{H}_3/\text{C}_5\text{H}_4$), 72.1 ($\text{C}_5\text{H}_3/\text{C}_5\text{H}_4$), 73.7 ($\text{C}_5\text{H}_3/\text{C}_5\text{H}_4$), 89.2 ($\text{C}_5\text{H}_3/\text{C}_5\text{H}_4$), 89.7 ($\text{C}_5\text{H}_3/\text{C}_5\text{H}_4$), 130.2 (CH=CH), 130.8 (CH=CH), 194.3

(C=O) ppm. FT-IR (KBr) ν : 1658 cm^{-1} (C=O). HRMS (ESI): m/z Found for $\text{C}_{15}\text{H}_{15}^{56}\text{FeO}$ [M+H]⁺ 267.04643 (Calc. 267.04668). Anal. Found: C, 67.93; H, 5.24. Calc. for $\text{C}_{15}\text{H}_{14}\text{FeO}$: C, 67.70; H, 5.30%. Chiral HPLC (Chiralcel AD-H, *n*-hexane:EtOH 98:2, 0.4 mL/min): 23.60 min (48.8%), 24.74 min (51.2%).

Compound (\pm)-**3** (the 1,3-isomer) was eluted as the third coloured band: red solid, yield: 207.0 mg (0.78 mmol, 47%). ¹H NMR (500 MHz, CDCl₃): δ 2.84 (ν_A) and 2.91 (ν_B) (part AB of ABX system, $J_{AX} = 8.0$ Hz, $J_{BX} = 7.5$ Hz, $J_{AB} = 15.0$, 2H, CH₂-CH=), 3.03 (ν_A) and 3.08 (ν_B) (part AB of ABX system, $J_{AX} = 7.5$ Hz, $J_{BX} = 7.5$ Hz, $J_{AB} = 15.0$, 2H, CH₂-CH=), 4.01-4.02 (m, 1H, C₅H₃/C₅H₄), 4.16-4.17 (m, 1H, C₅H₃/C₅H₄), 4.26-4.27 (m, 1H, C₅H₃/C₅H₄), 4.28-4.29 (m, 1H, C₅H₃/C₅H₄), 4.48 (dd, $J = 2.5$ Hz, 1.4 Hz, 1H, C₅H₃/C₅H₄), 4.65 (dd, $J = 2.6$ Hz, 1.3 Hz, 1H, C₅H₃/C₅H₄), 4.70-4.71 (m, 1H, C₅H₃/C₅H₄), 5.99-6.10 (m, 2H, overlapped X parts of two ABX systems, CH=), 9.84 (s, 1H, CHO) ppm. ¹³C {¹H} NMR (126 MHz, CDCl₃): δ 23.7 (CH₂-CH=), 24.1 (CH₂-CH=), 68.8 (C₅H₃/C₅H₄), 69.3 (C₅H₃/C₅H₄), 69.39 (C₅H₃/C₅H₄), 69.43 (C₅H₃/C₅H₄), 69.5 (C₅H₃/C₅H₄), 71.0 (C₅H₃/C₅H₄), 73.7 (C₅H₃/C₅H₄), 89.2 (C₅H₃/C₅H₄), 130.2 (CH=CH), 130.5 (CH=CH), 193.1 (C=O) ppm. FT-IR (KBr) ν : 1658 cm^{-1} (C=O). HRMS (ESI): m/z Found for $\text{C}_{15}\text{H}_{15}^{56}\text{FeO}$ [M+H]⁺ 267.04635 (Calc. 267.04668). Anal. Found: C, 68.18; H, 5.27. Calc. for $\text{C}_{15}\text{H}_{14}\text{FeO}$: C, 67.70; H, 5.30%. Chiral HPLC (Chiralcel OD-H, *n*-hexane:2-propanol 95:5, 0.8 mL/min): 20.68 min (49.9%), 26.19 min (50.1%).

4.3. The Vilsmeier reaction of **2**

DMF (104.2 mg, 113.0 μL , 1.46 mmol) and POCl₃ (167.5 mg, 100.0 μL , 1.09 mmol) were added to a solution of **2** (80.0 mg, 0.34 mmol) in chloroform (2.0 mL) The resulting solution was stirred for 20 h at room temperature, then quenched with saturated aq. Na₂CO₃ (10 mL) solution and stirred for 0.5 h at room temperature. The organic phase was separated, the aqueous phase was extracted with three times chloroform. The combined organic phases were washed with brine and dried over anhydrous Na₂SO₄. After removal of the volatiles under vacuum, the

residue was examined with ^1H NMR (CDCl_3) to reveal the presence of the two aldehydes (\pm)-**3** and (\pm)-**4** at the 4.0:1.0 ratio. View Article Online
DOI: 10.1039/D0DT01975E

4.4. Synthesis of alcohol (\pm)-**7**

Aldehyde (\pm)-**3** (100.0 mg, 0.376 mmol) was dissolved in THF (3.0 mL), then methanol (70 μL) and sodium borohydride (5.0 mg, 0.132 mmol) were added. The progress of the reaction was monitored by TLC. After 24 h methanol (70 μL) and sodium borohydride (5.0 mg, 0.132 mmol) were added again and the mixture was stirred until the substrate was consumed as judged from TLC (another 24 h). A saturated aqueous solution of NH_4Cl (50 mL) was added, the mixture was diluted with ethyl acetate and water, and extracted with ethyl acetate. The organic phase was washed with water and dried over MgSO_4 . The solution was evaporated to dryness and (\pm)-**7** was isolated from a saturated solution in hexanes as yellow, viscous oil (80.5 mg, 0.300 mmol, 80% yield). ^1H NMR (500 MHz, CDCl_3): δ 1.41 (bs, 1H, OH), 2.91 (bs, 4H, $\text{CH}_2\text{-CH=}$), 3.97 (bs, 1H, C_5H_3 or C_5H_4), 4.08-4.21 (m, 8H, C_5H_3 , C_5H_4 and CH_2OH), 5.97-6.05 (m, 2H, CH=) ppm. $^{13}\text{C}\{^1\text{H}\}$ NMR (126 MHz, CDCl_3): δ 23.9 ($\text{CH}_2\text{-CH=}$), 24.0 ($\text{CH}_2\text{-CH=}$), 60.4 (CH_2OH), 67.3 ($\text{C}_5\text{H}_3/\text{C}_5\text{H}_4$), 67.8 ($\text{C}_5\text{H}_3/\text{C}_5\text{H}_4$), 68.2 ($\text{C}_5\text{H}_3/\text{C}_5\text{H}_4$), 68.4 ($\text{C}_5\text{H}_3/\text{C}_5\text{H}_4$), 68.7 ($\text{C}_5\text{H}_3/\text{C}_5\text{H}_4$), 88.3 ($\text{C}_5\text{H}_3/\text{C}_5\text{H}_4$), 88.5 ($\text{C}_5\text{H}_3/\text{C}_5\text{H}_4$), 130.4 (CH=CH), 130.6 (CH=CH) ppm. HRMS (ESI): m/z Found for $\text{C}_{15}\text{H}_{16}^{56}\text{FeO}$ [M] $^+$ 268.05432 (Calc. 268.05451). Anal. Found C, 66.93; H 5.59. Calc. for $\text{C}_{15}\text{H}_{16}\text{FeO}$: C, 67.21; H 5.97%.

4.5. Synthesis of azide (\pm)-**8**

Alcohol (\pm)-**7** (100.0 mg, 0.373 mmol), sodium azide (145.0 mg, 2.230 mmol) and glacial acetic acid (5.0 mL) were placed in a flask and stirred at 50 $^\circ\text{C}$ for 3 h, then the reaction mixture was diluted with dichloromethane (5.0 mL) and saturated aq. NaHCO_3 (50 mL) was added. The phases were separated, the aqueous phase was extracted twice with dichloromethane. The combined organic phases were dried over Na_2SO_4 , and purified by column chromatography on silica gel (hexanes:ethyl acetate 25:2). A yellow band was collected that provided azide (\pm)-**8**

as an orange solid. Yield: 100.1 mg (0.341 mmol, 91%). ¹H NMR (500 MHz, CDCl₃): δ 2.93 (m, 4H, CH₂-CH=), 3.82-3.84 (m, 1H, C₅H₃/C₅H₄), 4.03-4.15 (overlapping m, 8H, C₅H₃, C₅H₄ and CH₂N₃), 6.01-6.04 (m, 2H, CH=) ppm. ¹³C{¹H} NMR (126 MHz, CDCl₃): δ 23.9 (CH₂-CH=), 24.0 (CH₂-CH=), 50.9 (CH₂N₃), 68.0 (C₅H₃/C₅H₄), 68.5 (C₅H₃/C₅H₄), 68.7 (C₅H₃/C₅H₄), 68.8 (C₅H₃/C₅H₄), 68.9 (C₅H₃/C₅H₄), 69.9 (C₅H₃/C₅H₄), 82.0 (C₅H₃/C₅H₄), 88.2 (C₅H₃/C₅H₄), 88.5 (C₅H₃/C₅H₄), 130.5 (CH=CH), 130.7 (CH=CH) ppm. HRMS (ESI): *m/z* Found for C₁₅H₁₅⁵⁶FeN₃ [M]⁺ 293.06073 (Calc. 293.06099). Anal. Found C, 61.93; H, 5.09; N, 14.11. Calc. for C₁₅H₁₅FeN₃: C, 61.48; H, 5.16; N, 14.33%.

4.6. Synthesis of (±)-**9**

The azide (±)-**8** (105.0 mg, 0.358 mmol) was dissolved in THF (8.0 mL) in a Schlenk flask and purged with argon. A solution of copper sulfate pentahydrate (4.5 mg, 0.018 mmol) and sodium ascorbate (21.3 mg, 0.011 mmol) in distilled water (2.0 mL) was added to the flask and degassed for 30 min under argon. 3-Propargyluracil (70.0 mg, 0.470 mmol) was added and the resulting mixture was stirred in the dark at room temperature for 4 days. Dichloromethane (15 mL) was added. The reaction mixture was washed three times with water, dried with anhydrous Na₂SO₄, and the volatiles were distilled off under vacuum. The product crystallized from CHCl₃/hexanes as a yellow solid (89.4 mg, 0.202 mmol, 56% yield). ¹H NMR (500 MHz, CDCl₃): δ 2.92 (d, *J* = 6.9 Hz, 4H, CH₂-CH=), 3.77-3.79 (m, 1H, C₅H₃), 4.05-4.14 (five multiplets, 5H, C₅H₃ and C₅H₄), 4.17 (app. s, 1H, C₅H₃ or C₅H₄), 5.15 (s, 2H, N-CH₂), 5.17 (s, 2H, N-CH₂), 5.72 (dd, *J* = 7.7, 1.4 Hz, 1H, 6-Ura), 5.99-6.03 (m, 2H, CH=CH), 7.17 (dd, *J* = 7.5, 5.7 Hz, 1H, 5-Ura), 7.53 (s, 1H, CH triazole), 9.09 (bs, 1H, NH) ppm. ¹³C{¹H} NMR (126 MHz, CDCl₃): δ 23.96 (CH₂-CH=), 24.01 (CH₂-CH=), 35.5 (CH₂), 50.1 (CH₂), 68.0 (C₅H₃/C₅H₄), 68.3 (C₅H₃/C₅H₄), 68.6 (C₅H₃/C₅H₄), 68.8 (C₅H₃/C₅H₄), 69.0 (C₅H₃/C₅H₄), 69.2 (C₅H₃/C₅H₄), 70.1 (C₅H₃/C₅H₄), 80.8 (C₅H₃/C₅H₄), 88.3 (C₅H₃/C₅H₄), 88.8 (C₅H₃/C₅H₄), 101.9 (CH Ura), 122.8 (CH triazole), 130.4 (CH=CH), 130.8 (CH=CH), 138.6 (CH Ura), 138.6 (C triazole) 151.9 (C=O Ura), 162.9

(C=O Ura) ppm. HRMS (ESI): m/z Found for $C_{22}H_{21}^{56}FeN_5O_2 [M]^+$ 443.10403 (Calc. 443.10392). Anal. Found C, 59.16; H, 5.09; N, 15.10. Calc. for $C_{22}H_{21}FeN_5O_2$: C, 59.61; H, 4.78; N, 15.80%.

4.7. Synthesis of **9a**

Compound **9a** was obtained similarly as described recently.¹⁹ 1H NMR (500 MHz, $CDCl_3$): δ 4.17 (s, 5H, C_5H_5), 4.21 (s, 2H, C_5H_4), 4.28 (s, 2H, C_5H_4), 5.16 (s, 2H, N- CH_2), 5.22 (s, 2H, N- CH_2), 5.72 (d, $J = 7.5$ Hz, 1H, 6-Ura), 7.20 (app. t, 1H, 5-Ura), 7.52 (bs, 1H, CH triazole), 9.31 (bs, 1H, NH) ppm. $^{13}C\{^1H\}$ NMR (126 MHz, $CDCl_3$): δ 35.4 (CH_2), 50.0 (CH_2), 68.9 (C_5H_4), 67.0 (C_5H_5), 69.0 (C_5H_4), 80.8 (C_5H_4), 101.7 (CH Ura), 122.9 (CH triazole), 139.0 (CH Ura), 142.8 (C triazole), 152.2 (C=O Ura), 163.0 (C=O Ura) ppm. HRMS (ESI): m/z Found for $C_{18}H_{18}^{56}FeN_5O_2 [M+H]^+$ 392.08004 (Calc. 392.08044).

4.8. Crystal structure determination

Single-crystals of (*R_p*)-**3** and (*R_p*)-**4** suitable for X-ray analyses were grown from racemic samples in hexanes at -20 °C. The X-ray diffraction measurements of both compounds were carried out on a Rigaku Oxford Diffraction SuperNova instrument equipped with microfocus Cu X-ray source. During the measurements crystals were maintained at 100 K with the use of Oxford Cryosystems nitrogen gas-flow device. Unit-cell parameter determination and raw diffraction image processing were performed with the native diffractometer software. All structures were solved using a charge-flipping method implemented in the *SUPERFLIP* program^{31,32} and refined with the *JANA* package³³ within the independent atom model approximation. Scattering factors, in their analytical form, were taken from the International Tables for Crystallography.³⁴ Final crystal, data collection and refinement parameters for all compounds are summarized in associated CIF files, which are present in the Supporting Information, or can be retrieved from the Cambridge Structural Database³⁵ (deposition numbers: CCDC 1935549-50).

4.9. Biological studies

View Article Online
DOI: 10.1039/D0DT01975E

The MCF-7, MDA-MB-231, and A549 cell lines were cultured in DMEM with high glucose medium (Lonza, Basel, Switzerland) supplemented with 10% fetal bovine serum (EuroClone, Sizzano, Italy), 2mM L-glutamine, antibiotics (100 U/ml penicillin, 100 µg/ml streptomycin, Sigma-Aldrich, St. Louis, MO, USA) and 10 µg/ml of human recombinant insulin (Sigma-Aldrich) for MCF-7 at 37 °C with 5% CO₂. MRC-5 human fibroblasts were cultured in MEME (Sigma-Aldrich) supplemented with 10% fetal bovine serum (EuroClone), 2mM L-glutamine, antibiotics (100 U/ml penicillin, 100 µg/ml streptomycin) and non-essential amino acids (Sigma-Aldrich). The cell viability after exposure to the newly synthesized compounds were tested by MTT assay. Before the treatment, cells were trypsinized in 0.25% trypsin-EDTA solution (Sigma-Aldrich) and seeded into 96-well microplates at 6 x 10³ cells/well. The cells were treated with tested compounds at the appropriate concentrations in DMSO at 0.5% final concentration 24 h after plating. After 72 h incubation with compounds or carrier, supernatants were discarded and subsequently MTT stock solution (Sigma-Aldrich) was added to each well to a final concentration of 1 mg/mL. After 1 h of incubation at 37 °C, water-insoluble dark blue formazan crystals were dissolved in DMSO (200 µL) (37 °C/10 min incubation). Optical densities were measured at 570 nm using BioTek microplate reader. All measurements were carried out in tetraplicate and the results are expressed in percentage of cell viability relative to control (cells without inhibitor in 0.5% DMSO).

The β-galactosidase activity was stained in MCF-7 cell line with used Senescence β-Galactosidase Staining Kit (Cell Signaling Technology) according to manufacturer's protocol. Etoposide, used as a positive control, was obtained from Sigma-Aldrich. Images were generated using bright field by Olympus inverted microscope (Olympus inverted microscope CK X41, 20x objective, U-TV0.63XC Olympus Camera; Olympus, Tokyo, Japan).

Supporting Information

Additional figures and tables, HPLC traces, experimental details for the resolution of (\pm)-**3**,
crystallographic data. New Article Online
DOI: 10.1039/D0DT01975E

Conflicts of interest

There are no conflicts to declare.

Acknowledgements

The authors thank the National Science Centre for financial support of this work (grant No 2015/17/B/ST5/00547) and Warsaw University of Technology. The X-ray diffraction experiments were carried out at the Department of Physics, University of Warsaw, on the Rigaku Oxford Diffraction SuperNova diffractometer, which was co-financed by the European Union within the European Regional Development Fund (POIG.02.01.00-14-122/09).

References and notes

- 1 For reviews see: (a) W. Heo, T. R. Lee, *J. Organomet. Chem.*, 1999, **578**, 31-42; (b) D. E. Herbert, U. F. J. Mayer, I. Manners, *Angew. Chem. Int. Ed.*, 2007, **46**, 5060-5087; (c) R. A. Musgrave, A. D. Russell, I. Manners, *Organometallics*, 2013, **32**, 5654-5667.
- 2 (a) A. J. Locke, C. Jones, C. J. Richards, *J. Organomet. Chem.*, 2001, **637-639**, 669-676; (b) M. Ogasawara, T. Nagano, T. Hayashi, *J. Am. Chem. Soc.*, 2002, **124**, 9068-9069.
- 3 For general reviews on olefin metathesis in transition metal complexes, see: (a) E. B. Bauer, J. A. Gladysz, in *Handbook of Metathesis*, ed. R. H. Grubbs, Wiley-VCH, Weinheim, 1st. edition, 2003, Vol. 2, 2.11, pp. 403-431; (b) A. Pietrzykowski, W. Buchowicz, in *Advances in Organometallic Chemistry and Catalysis: The Silver/Gold Jubilee International Conference on Organometallic Chemistry Celebratory Book*, ed. A. J. L. Pombeiro, J. Wiley & Sons, 2014, 12, pp. 157-170; (c) T. Fiedler, J. A. Gladysz, in *Olefin Metathesis: Theory and Practice*, ed. K. Grela, John Wiley & Sons, 2014, 9, pp. 311-328.
- 4 For recent examples of olefin metathesis in metallocenes see: (a) T. A. Tumay, G. Kehr, R. Fröhlich, G. Erker, *Dalton Trans.*, 2009, 8923-8928; (b) M. Ogasawara, S. Watanabe, K.

Nakajima, T. Takahashi, *J. Am. Chem. Soc.*, 2010, **132**, 2136-2137; (c) W. Buchowicz, A. Furmańczyk, J. Zachara, M. Majchrzak, *Dalton Trans.*, 2012, **41**, 9269-9271; (d) M. Ogasawara, W.-Y. Wu, S. Arae, K. Nakajima, T. Takahashi, *Organometallics*, 2013, **32**, 6593–6598; (e) S. Arae, K. Nakajima, T. Takahashi, M. Ogasawara, *Organometallics*, 2015, **34**, 1197-1202.

5 For recent reviews see: (a) A. Nguyen, A. Vessières, E. A. Hillard, S. Top, P. Pigeon, G. Jaouen, *Chimia*, 2007, **61**, 716-724; (b) C. Ornelas, *New J. Chem.*, 2011, **35**, 1973-1985; (c) S. S. Braga, A. M. S. Silva, *Organometallics*, 2013, **32**, 5626-5639; (d) R. Wang, H. Chen, W. Yan, M. Zheng, T. Zhang, Y. Zhang, *Eur. J. Med. Chem.*, 2020, **190**, 112109.

6 Selected recent examples: (a) G. Tabbi, C. Cassina, G. Cavigiolio, D. Colangelo, A. Ghiglia, L. Viano, D. Osella, *J. Med. Chem.*, 2002, **45**, 5786-5796; (b) P. James, J. Neudörfl, M. Eissmann, P. Jesse, A. Prokop, H.-G. Schmalz, *Org. Lett.*, 2006, **8**, 2763-2766; (c) K. Kowalski, A. Koceva-Chyla, A. Pieniżek, J. Bernasińska, J. Skiba, A. J. Rybarczyk-Pirek, Z. Józwiak, *J. Organomet. Chem.*, 2012, **700**, 58-68; (d) A. Hottin, D. W. Wright, A. Steenackers, P. Delannoy, F. Dubar, C. Biot, G. J. Davies, J.-B. Behr, *Chem. Eur. J.*, 2013, **19**, 9526-9533; (e) H. V. Nguyen, A. Sallustrau, J. Balzarini, M. R. Bedford, J. C. Eden, N. Georgousi, N. J. Hodges, J. Kedge, Y. Mehellou, C. Tselepis, J. H. R. Tucker, *J. Med. Chem.*, 2014, **57**, 5817-5822; (f) Y. Wang, P. Pigeon, S. Top, M. J. McGlinchey, G. Jaouen, *Angew. Chem. Int. Ed.*, 2015, **54**, 10230-10233.

7 (a) D. Plažuk, A. Vessières, E. A. Hillard, O. Buriez, E. Labbé, P. Pigeon, M.-A. Plamont, C. Amatore, J. Zakrzewski, G. Jaouen, *J. Med. Chem.*, 2009, **52**, 4964-4967; (b) M. Gormen, D. Plažuk, P. Pigeon, E. A. Hillard, M.-A. Plamont, S. Top, A. Vessières, G. Jaouen, *Tetrahedron Lett.*, 2010, **51**, 118-120; (c) M. Gormen, P. Pigeon, S. Top, A. Vessières, M.-A. Plamont, E. A. Hillard, G. Jaouen, *Med. Chem. Commun.*, 2010, **1**, 149-151; (d) M. Gormen, P. Pigeon, S. Top, E. A. Hillard, M. Huché, C. G. Hartinger, F. de Montigny, M.-A. Plamont, A. Vessières,

- G. Jaouen, *ChemMedChem*, 2010, **5**, 2039-2050; (e) M. Görmen, P. Pigeon, E. A. Hillard, A. Vessières, M. Huché, M.-A. Richard, M. J. McGlinchey, S. Top, G. Jaouen, *Organometallics*, 2012, **32**, 5856-5866; (f) Y. L. K. Tan, P. Pigeon, S. Top, E. Labbé, O. Buriez, E. A. Hillard, A. Vessières, C. Amatore, W. K. Leong, G. Jaouen, *Dalton Trans.*, 2012, **41**, 7537-7549; (g) J. de Jesus Cázares-Marinero, O. Buriez, E. Labbé, S. Top, C. Amatore, G. Jaouen, *Organometallics*, 2013, **32**, 5926-5934; (h) M. Beauperin, S. Top, M.-A. Richard, D. Plažuk, P. Pigeon, S. Toma, V. Poláčková, G. Jaouen, *Dalton Trans.*, 2016, **45**, 13126-13134.
- 8 D. R. van Staveren, N. Metzler-Nolte, *Chem. Rev.*, 2004, **104**, 5931-5985.
- 9 (a) K. Schlögl, in *Topics in Stereochemistry*, ed. N. L. Allinger, E. L. Eliel, Wiley, Hoboken, 1967, *Stereochemistry of Metallocenes*, pp. 39-91; (b) D. Schaarschmidt, H. Lang, *Organometallics*, 2013, **32**, 5668-5704.
- 10 T. H. Barr, E. S. Bolton, H. L. Lentzner, W. E. Watts, *Tetrahedron*, 1969, **25**, 5245-5253.
- 11 (a) M. Hisatome, T. Sakamoto, K. Yamakawa, *J. Organomet. Chem.*, 1976, **107**, 87-101; (b) R. G. Sutherland, J. R. Sutton, W. H. Horspool, *J. Organomet. Chem.*, 1976, **122**, 393-401; (c) M. Hisatome, N. Watanabe, T. Sakamoto, K. Yamakawa, *J. Organomet. Chem.*, 1977, **125**, 79-93.
- 12 M. Hillman, L. Matyevich, E. Fujita, U. Jagwani, J. McGowan, *Organometallics*, 1982, **1**, 1226-1229.
- 13 D. R. Talham, D. O. Cowan, *Organometallics*, 1987, **6**, 932-937.
- 14 A. Reichert, M. Bolte, H.-W. Lerner, M. Wagner, *J. Organomet. Chem.*, 2013, **744**, 15-23.
- 15 C. Nilewski, M. Neumann, L. Tebben, R. Fröhlich, G. Kehr, G. Erker, *Synthesis*, 2006, **13**, 2191-2200.
- 16 J.-H. Jia, X.-M. Tao, Y.-J. Li, W.-J. Sheng, L. Han, J.-R. Gao, Y.-F. Zheng, *Chem. Phys. Lett.*, 2011, **514**, 114-118.

- 17 (a) G. D. Broadhead, J. M. Osgerby, P. L. Pauson, *J. Chem. Soc.*, 1958, 650-656; (b) S. Movahhed, J. Westphal, M. Dindaroğlu, A. Falk, H.-G. Schmalz, *Chem. Eur. J.*, 2016, **22**, 7381-7384.
- 18 O. Riant, O. Samuel, H. B. Kagan, *J. Am. Chem. Soc.*, 1993, **115**, 5835-5836.
- 19 A. Kasprzak, M. Koszytkowska-Stawińska, A. Nowicka, W. Buchowicz, M. Popławska, *J. Org. Chem.*, 2019, **84**, 15900-15914.
- 20 P. V. Solntsev, K. L. Spurgin, J. R. Sabin, A. A. Heikal, V. N. Nemykin, *Inorg. Chem.*, 2012, **51**, 6537-6547.
- 21 D. Paliwoda, M. Hanfland, A. Katrusiak, *J. Phys. Chem.*, 2019, **C 123**, 25719-25723.
- 22 A. Hottin, A. Scandolera, L. Duca, D. W. Wright, G. J. Davies, J. B. Behr, *Bioorg. Med. Chem. Lett.*, 2016, **26**, 1546-1549.
- 23 Taking into account that ferroquine (a 1,2-unsymmetrically disubstituted planar-chiral ferrocene derivative) has been usually applied in biological studies as a racemate, we decided to test racemic (\pm)-**9**. We presume that the main role of the ferrocenyl moiety is production of reactive oxygen species. Thus, we do not expect a significant chiral effect.
- 24 (a) K. Kowalski, J. Skiba, L. Oehninger, I. Ott, J. Solecka, A. Rajnisz, B. Therrien, *Organometallics*, 2013, **32**, 5766-5773; (b) J. Skiba, K. Kowalski, A. Prochnicka, I. Ott, J. Solecka, A. Rajnisz, B. Therrien, *J. Organomet. Chem.*, 2015, **782**, 52-61.
- 25 M. Maschke, M. Lieb, N. Metzler-Nolte, *Eur. J. Inorg. Chem.*, 2012, 5953-5959.
- 26 (a) G. Jaouen, A. Vessières, S. Top, *Chem. Soc. Rev.*, 2015, **44**, 8802-8817; (b) Y. Wang, P. M. Dansette, P. Pigeon, S. Top, M. J. McGlinchey, D. Mansuy, G. Jaouen, *Chem. Sci.*, 2018, **9**, 70-78.
- 27 A. Litwiniec, A. Grzanka, A. Helmin-Basa, L. Gackowska, D. Grzanka, *J. Cancer Res Clin Oncol*, 2010, **136**, 717-736.

- 28 Y. Wang, Y. Wang, S. Liu, Y. Liu, H. Xu, J. Liang, J. Zhu, G. Zhang, W. Su, W. Dong, Q. Guo, *Biomed Pharmacother*, 2018, **107**, 606-614.
- 29 D. D. Perrin, W. L. F. Armarego, *Purification of Laboratory Chemicals*, Pergamon Press, New York, 1988.
- 30 J. M. Casas-Solvas, A. Vargas-Berenguel, L. F. Capitán-Vallvey, F. Santoyo-González, *Org. Lett.*, 2004, **6**, 3687-3690.
- 31 (a) G. Oszlányi, A. Sütő, *Acta Cryst. Sect. A*, 2004, **60**, 134-141; (b) G. Oszlányi, A. Sütő, *Acta Cryst. Sect. A*, 2005, **61**, 147-152.
- 32 (a) L. Palatinus, G. Chapuis, *J. Appl. Cryst.*, 2007, **40**, 786-790; (b) L. Palatinus, *Acta Cryst. Sect. B*, 2013, **69**, 1-16.
- 33 V. Petříček, M. Dušek, L. Palatinus, *Z. Kristallogr.*, 2014, **229**, 345-352.
- 34 E. Prince, in *International Tables for Crystallography, Volume C: Mathematical, physical and chemical tables*, International Union of Crystallography, Chester, UK, 2006.
- 35 C. R. Groom, I. J. Bruno, M. P. Lightfoot, S. C. Ward, *Acta Cryst. Sect. B*, 2016, **72**, 171-179.

Table of contents entryView Article Online
DOI: 10.1039/D0DT01975E

Ansa-ferrocenealdehyde, obtained by formylation of a metathesis-derived *ansa*-ferrocene, was transformed into a conjugate with triazole and uracil with anticancer activity.

